Chapter 3

Hazard and Risk Assessment of Workplace Exposure to Engineered Nanoparticles: Methods, Issues, and Carbon Nanotube Case Study

Eileen Kuempel and Vincent Castranova

CHAPTER OUTLINE

3.1 Introduction 65
- 3.1.1 Risk Assessment Paradigm 66
- 3.1.2 Hazard Assessment 67
- 3.1.3 Dose–Response Assessment 71
  - *No Observed or Lowest Observed Adverse Effect Levels 71*
  - *Benchmark Dose Methods 72*
  - *Comparison of BMD versus NOAEL/LOAEL 73*
- 3.1.4 Temporal Extrapolation 73

3.2 Case Study Example: Carbon Nanotubes 74
- 3.2.1 Data Description 74
- 3.2.2 Severity of Effects 75
- 3.2.3 Risk Assessment Steps: Benchmark Dose Estimation 77

3.3 Discussion 83
- 3.3.1 Comparison to Other Methods 83
- 3.3.2 Research Needs 87
- 3.3.3 Future Directions 88

3.4 Appendix: Pulmonary Ventilation Rate Calculations 89
- 3.4.1 Rat Ventilation Rate 90
- 3.4.2 Human Ventilation Rate 90

3.1 INTRODUCTION

Toxicology data from experimental studies in animals are frequently used in risk assessment when human dose–response data are not available.

Assessing Nanoparticle Risks to Human Health. DOI: 10.1016/B978-1-4377-7863-2.00003-0

Collaborations among industrial hygienists, toxicologists, risk assessors, and other disciplines provide an opportunity to develop an improved scientific data basis for assessing the risk of exposure to nanomaterials. In this chapter, the components of the risk assessment process are described, with focus on occupational risk assessment of inhaled particles. A case study is presented using rat subchronic inhalation data of multiwalled carbon nanotubes (MWCNT) (Ma-Hock et al., 2009; Pauluhn, 2010a) to illustrate the application of risk assessment methods to engineered nanoparticles using currently available data. Issues in using these data in quantitative risk estimation are discussed, as are research needs to reduce the uncertainties in the risk assessment of occupational exposure to nanomaterials.

3.1.1 Risk Assessment Paradigm

Risk assessment is a process to systematically characterize the scientific evidence of potential adverse health effects from human exposures to hazardous agents (NRC, 1983). The traditional risk assessment framework developed in the United States, and used in various forms worldwide, includes four main steps: (1) hazard assessment, (2) dose–response assessment, (3) exposure assessment, and (4) risk characterization (NRC, 1983). Research studies in various fields including toxicology, exposure measurement, and computational methods are needed to provide the data for risk assessment in order to inform risk management decision-making. Risk communication and processes to obtain stakeholder input are integral components of the risk assessment process. In many cases, sufficient data are not available for a full risk characterization, and risk management decisions may need to be made based on limited available data. A higher level of precaution in controlling exposures is prudent when the extent of the hazard is not well known, as with many nanomaterials (Schulte and Salamanca-Buentello, 2007).

This classic risk assessment paradigm was recently re-evaluated by the National Research Council (NRC) in response to a charge from the US EPA to recommend improvements to the risk assessment process as practiced (NRC, 2009). In its report, the NRC recommended retaining the four basic steps of the risk assessment process and also recommended additional steps to improve the utility of risk assessment and the technical analyses supporting risk assessment. Among these, the NRC proposed adding an initial step in problem formulation and scoping, as well as revisions to the risk management phase to evaluate both risk and nonrisk information (e.g., technical feasibility) in a systematic evaluation of potential options. Toward the goal of improving the utility of risk assessment, the revised NRC framework explicitly asks what options are available to reduce the hazards or exposures that have been identified, and how can risk assessment be used to evaluate the merits of the various options (NRC, 2009).

In the absence of epidemiology data for workers exposed to engineered nanoparticles, much of the current focus in risk assessment involves toxicology studies in animals to assess the hazard, determine dose–response and time–course relationships, and identify modes of action. The design of toxicology research studies for use in risk assessment necessitates an interface between toxicology and risk assessment to develop adequate data for qualitative and quantitative analyses. Evaluating the key information needs in this process provides an opportunity to focus additional research efforts to the generation of data necessary to reduce uncertainties in estimating the hazard and risk of exposure to nanoparticles. As with workers exposed to other chemicals or particles, nanotechnology workers are likely to have the highest exposures and greatest potential for adverse health effects associated with the production of nanoparticles and their use in commercial applications. The hazard and dose–response assessment steps are discussed further in the following sections, as these steps are used in the quantitative risk assessment. The exposure assessment step (which is beyond the scope of this chapter) is needed to characterize the risk in a given population.

3.1.2 **Hazard Assessment**

The hazard assessment seeks to identify the nature of any hazardous effects and the evidence regarding the biological mode of action. Many of the same adverse lung responses previously reported following inhalation of fibers or fine particles are being found with exposure to nanoparticles, although often at lower mass doses due to the increased total particle surface area (Driscoll, 1996; Oberdörster and Yu, 1990; Sager and Castranova, 2009; Sager et al., 2008) or volume (Bellmann et al., 1991; Oberdörster et al., 1992; Pauluhn, 2010a) per unit mass for nanoparticles compared to their fine-sized analogues. Poorly soluble nanoparticles (e.g., metal oxides such as titanium dioxide and aluminum oxide) have been shown to cause greater inflammation response in rodent lungs than the same mass of larger-sized respirable particles of the same chemical composition (Bermudez et al., 2002, 2004; Oberdörster and Ferin, 1992; Sager et al., 2008) and in *in vitro* cell assays (Rushton et al., 2010). Common pathways for the pulmonary pathogenicity of inhaled particles of varying sizes and shapes include direct cytotoxicity (e.g., due to reactive surfaces), activation of oxidant release from phagocytes, and secretion of inflammatory cytokines and/or proliferative factors (Castranova, 1998, 2000; Donaldson et al., 1996; Oberdörster et al., 2005). These pathogenic pathways have been linked to rat lung tumorigenesis associated with chronic exposures to various types and sizes of poorly soluble particles, apparently by a mode of action involving indirect (secondary) genotoxicity due to the earlier

Table 3.1 Hazard Data Examples: Rodent Studies of Single-Walled Carbon Nanotubes (SWCNT)

Response	Dose and Duration[a]	Species and Exposure Route[b]	Reference
Pulmonary inflammation Granulomas	0.1 or 0.5 mg per mouse (7 and 90 day pe)	Mouse ($B6C3F_1$, male); IT	Lam et al. (2004)
Cell proliferation – lung epithelial cells	0.4 mg per rat (1 and 21 day pe)	Rat (F344, female); PA	Mangum et al. (2006)
Pulmonary fibrosis (early onset and persistent)	5, 10, 20, 40 μg per mouse (1, 3, 7, 28, and 56 day pe)	Mouse (C57BL/6, female); PA	Shvedova et al. (2005)
K-ras oncogene mutations in lung tissue	5 mg/m^3 (5 h/day, 4 day); 1, 7, and 28 day pe	Mouse (C57BL/6), female; inhalation (whole body)	Shvedova et al. (2008)
Cardiovascular – oxidative stress and plaque formation	20 μg per mouse every 2 weeks for 10 weeks (7, 28, and 56 day pe)	Mouse (C57BL/6, male); PA	Li et al. (2007)

[a] *In addition to 0 dose (control); pe, postexposure.*
[b] *IT, intratracheal instillation; PA, pharyngeal aspiration.*

inflammatory and proliferative events (Baan, 2007; Castranova, 2000; ILSI, 2000; Schins and Knaapen, 2007).

Persistent granulomatous inflammation and interstitial fibrosis are also among the responses observed in rodents exposed to MWCNT or single-walled carbon nanotubes (SWCNT) by various routes of exposure (intratracheal instillation (IT), pharyngeal aspiration (PA), or inhalation) (Tables 3.1 and 3.2). In addition, pulmonary exposure to SWCNT has been associated with oxidative stress and enhanced plaque formation in the aorta, while intraperitoneal exposure to MWCNT has been linked to mesothelioma in some studies (Tables 3.1 and 3.2). MWCNT and SWCNT have been shown in several studies to be more potent on a mass basis (i.e., a lower dose associated with a given adverse lung response, or a greater adverse response at a given dose) compared to ultrafine carbon black (Table 3.3) and other poorly soluble particles including silica and asbestos (Elder et al., 2006; Lam et al., 2004; Muller et al., 2005; Shvedova et al., 2005). In contrast to the metal oxides, cellular responses to carbon nanotubes (CNT) are not well predicted by the reactive oxygen species generation; rather, the nanostructured CNT appear to act as a basement membrane substrate that enhances fibroblast proliferation and collagen production *in vitro*. *In vivo*, this would result in thickening of the alveolar septal air/blood barrier and a decrease in gas exchange between lung and blood (Wang et al., 2010).

Some types of MWCNT and SWCNT have also been shown to elicit similar biological effects as fibers, in that the longer, thinner structures are more

Table 3.2 Hazard Data Examples: Rodent Studies of Multiwalled Carbon Nanotubes (MWCNT)

Response	Dose and Duration[a]	Species and Exposure Route[b]	Reference
Granulomatous inflammation	0.1, 0.5, 2.5 mg/m^3 (6 h/day, 5 d/week, for 13 week)	Rat (Wistar, male); inhalation (head and nose)	Ma-Hock et al. (2009)
Lipoproteinosis			
Pulmonary inflammation and fibrosis	0.1, 0.45, 1.68, 5.98 mg/m^3 (6 h/day, 5 d/week, for 13 week)	Rat (Wistar, male); inhalation (nose-only)	Pauluhn (2010a)
Pulmonary inflammation and fibrosis	0.5, 2, 5 mg per rat (28 and 60 day pe)	Rat (Sprague Dawley, Wistar, female); IT	Muller et al. (2005, 2008)
Bronchiolitis obliterans	12.5 mg per guinea pig (3 month pe)	Guinea pig (three-color, male); IT	Grubek-Jaworskaa et al. (2006)
Peribronchial fibrosis			
Granulomatous inflammation	10, 20, 40, 80 µg per mouse (1, 7, 28, 56 day pe)	Mouse (C57BL/6, male); PA	Porter et al. (2010)
Pulmonary fibrosis			
Mesothelioma	3 mg (25 week pe)	Mouse (p53(+/−, m)	Takagi et al. (2008)
No mesothelioma	2, 20 mg (2 year pe)	Rat (Wistar, m)	Muller et al. (2009)
Inflammation, by length	50 µg (1, 7 day pe)	Mouse (C57B1/6, f)–all IP	Poland et al. (2008)

[a] *In addition to 0 dose (control); pe: postexposure.*
[b] *IP, intraperitoneal injection; IT, intratracheal instillation; PA, pharyngeal aspiration.*

Table 3.3 Adverse Effect Levels in Rats after Subchronic (13-week) Inhalation Exposure to Carbon Particles and Carbon Nanotubes

Study	Compound	Effect Level in Rats		Effect
		NOAEL (mg/m^3)	LOAEL (mg/m^3	
Elder et al. (2006)	Ultrafine carbon black (Printex 90)	1	7	Pulmonary inflammation
Ma-Hock et al. (2009)	Multiwalled carbon nanotubes (BASF, Nanocyl)	nd	0.1	Granulomatous inflammation
		.0.1	.0.5	Alveolar proteinosis
Pauluhn et al. (2010a)	Multiwalled carbon nanotubes (Baytubes®, Bayer)	0.1	0.45	Pulmonary inflammation Alveolar septal thickening

LOAEL: Lowest observed adverse effect level.
NOAEL: No observed adverse effect level.

inflammogenic (Poland et al., 2008) and can penetrate from the lung subpleural tissue to the intrapleural space (Mercer et al., 2010). SWCNT and MWCNT have been shown to interfere with normal cell division in cell culture systems (Muller et al., 2008; Sargent et al., 2009). MWCNT can cause the

two normal centrosomes to cluster, forming a single pole. The resulting mitotic spindles are monopolar rather than bipolar (Sargent et al., 2011). In addition, MWCNT have been reported to form cross bridges between multiple cell nuclei after pulmonary exposure (Muller et al., 2008). In contrast, SWCNT appear to fragment centrosomes, causing multipolar mitotic spindle formation, abnormal chromosome division, and aneuploidy (Sargent et al., 2009). In comparison, chrysotile asbestos also interferes with the normal mitotic process but not by binding to centrosomes. Rather, asbestos fibers interact with mitotic spindles and interfere with cytokinesis by forming bridges to prevent normal separation of daughter nuclei (Asakura et al., 2010). MWCNT have also been shown to translocate from the lungs to the mesothelial tissue lining the lung (Mercer et al., 2010), to lung-associated lymph nodes (as do other inhaled particles), and to other organs including liver and kidneys, with tissue damage observed in those organs (Reddy et al., 2010). Other nanoparticles (e.g., silver, iridium) have also been shown to translocate from the lungs via the systemic circulation to other organs and tissues (Semmler et al., 2004; Semmler-Behnke et al., 2007; Takenaka et al., 2001).

Compared to larger particles, some unique observations for nanoparticles include their ability to enter and interact with cells and cell organelles. Individual nanoparticles of titanium dioxide have been observed inside cell organelles including the cell nucleus (Geiser et al., 2005) and mitochondria, which can disrupt mitochondrial and cellular function (Li et al., 2003). In addition, Mercer et al. (2010) have published electron micrographs showing individual MWCNT within alveolar macrophages and epithelial cells. Spherical nanoparticles depositing in the nasal region have been shown to enter the brain via neuronal transport in the rat and cause inflammation in the olfactory bulb (Elder et al., 2006; Oberdörster et al., 2002; Oberdörster et al., 2009).

The nature of the hazard and mode of action influence the extent to which information on larger particles of the same chemical composition or surface reactivity can be reliably extrapolated to nanoparticles. In the case of poorly soluble particles, a relationship between the particle surface area dose of nanoscale or larger particles and pulmonary inflammation or other adverse lung effects (including rat lung tumors in chronic studies) has been reported (Driscoll, 1996; Oberdörster and Yu, 1990; Sager and Castranova, 2009; Sager et al., 2008). Therefore, utilizing the available data for other particles and fibers may facilitate hazard and risk characterization for classes of materials with common modes of action. However, additional data are needed to link the potential biological effects of the vast number of nanomaterials to given physical–chemical properties (Rushton et al., 2010) in order to develop predictive hazard/risk grouping strategies.

3.1.3 Dose–Response Assessment

The essential data basis for quantitative risk assessment is the dose–response relationship. If epidemiological data are available, these studies are generally preferred for risk assessment since there is no uncertainty about extrapolation across species or about the species-relevance of the response end point. However, quantitative exposure data are often not available in epidemiology studies, and in the case of nanoparticles no epidemiology studies have been reported. Thus, experimental data in animals are used to examine the dose–response relationships. Standard methods of risk assessment involve determination of either an adverse effect level (no or lowest observed) or a benchmark dose estimate. In either case, the animal dose must be extrapolated to humans, either by allometric scaling (i.e., based on body weight) or by using other data available on the factors that influence the target tissue dose in each species (i.e., adsorption, distribution, metabolism, elimination). A potentially useful metric to scale human versus animal dose when evaluating pulmonary exposure–response is deposited dose per surface area of alveolar epithelium (as described in sections 3.2.3 and 3.3.1).

No Observed or Lowest Observed Adverse Effect Levels

A lowest observed adverse effect level (LOAEL) or no observed adverse effect level (NOAEL) approach has often been used for noncarcinogenic agents that are assumed to act through a threshold mechanism such that exposures below that threshold dose would not be expected to cause an adverse effect. In this approach, after extrapolation from animals to humans, the NOAEL or LOAEL is typically divided by adjustment factors to account for uncertainty in extrapolating the animal data to humans, inter-individual variability in the distribution of human responses, subchronic to chronic data extrapolation, and/or use of a LOAEL versus a NOAEL. Factors of 10 each have typically been used in the absence of other data (EPA, 2000). These adjustment factors (a.k.a. uncertainty or safety factors) are intended to provide a sufficient margin of safety to be associated with virtually zero risk of adverse effect in the population if exposures are kept below the calculated exposure limits. However, a threshold assumption may not be applicable (e.g., if exposure to a hazardous agent adds to a response associated with another environmental exposure or to background disease processes or incidence) and may not adequately account for inter-individual variation in a population (NRC, 2009; White et al., 2009). Thus, a benchmark dose method is often preferred to provide quantitative risk estimates and to demonstrate the health benefits of reducing exposures (e.g., in the context of regulatory decision-making; US Supreme Court, 1980).

Benchmark Dose Methods

If sufficient dose–response data are available, benchmark dose (BMD) estimation is often preferred to a NOAEL or LOAEL (Crump, 1984, 1995; EPA, 2000). A BMD is a risk-associated dose estimated by model curve fitting to the dose–response data. BMD estimates have been used in both cancer and noncancer risk assessments. Relevant examples include pulmonary responses to inhaled fine and nanoscale (ultrafine) particles (Dankovic et al., 2007; Kuempel et al., 2006).

A benchmark dose is defined as "...a statistical lower confidence limit for the dose corresponding to a specified small increase in level of [adverse] health effect over the background level" (Crump, 1984). In practice, the term "benchmark dose" is often used for the maximum likelihood estimate (MLE), while BMD(L) is the lower 95% confidence limit of the BMD. The benchmark response (BMR) is the adverse response level associated with the BMD(L). A BMR is typically in the low region of the dose–response data, for example, a 10% response, which is near the statistical lower limit of detection in an animal bioassay. For dichotomous (yes/no) response data, a BMD can be defined as the dose associated with either an extra risk (relative to the background probability of having a normal response) or an excess risk (additional probability above background) (Crump, 2002). Excess risk is used in the example in this chapter because it provides an estimate of the exposure-attributable risk. The BMD is calculated as the dose d corresponding to the specified excess risk in the proportion of animals with a given adverse lung response (BMR):

$$\text{BMR} = P(d) - P(0) \tag{3.1}$$

where $P(d)$ is the probability of an adverse response at the BMD and $P(0)$ is the probability of that adverse response in an unexposed population (Crump, 2002; EPA, 2006).

BMD methods and models are also available for continuous response data (Crump, 1995, 2002; EPA, 2010), although a detailed discussion is beyond the scope of the chapter. Briefly, BMD estimation using continuous data requires specifying a BMR level along a continuum of responses. Continuous response measures may be associated with normal biological structure or function that can be perturbed in response to a toxicant and eventually result in a functional impairment. Toxicology studies can provide dose–response data for quantitative risk assessment based on continuous responses, as well as information on the biologically relevant level of response in animals and humans.

Comparison of BMD versus NOAEL/LOAEL

There are several advantages of BMD methods over the NOAEL/LOAEL approach. First, the BMD curve fitting uses all the data in the dose–response relationship, not just a single data point. Second, although the NOAEL and LOAEL doses are dependent on the particular dose groups and spacing selected for the study (and tend to be higher in studies with fewer observations), the BMD method can provide dose estimates at a constant level of risk (e.g., 10%) for better comparison across studies. Third, the BMD method takes appropriate statistical account of the sample size and provides estimates of the confidence limits on the BMD estimates. Fourth, although the NOAEL or LOAEL approach assumes a threshold response regardless of the shape of the dose–response relationship, BMD(L)s are risk estimates derived from a statistical model fit to the dose–response data. A comparison of NOAELs and BMDs showed that the estimated risk associated with NOAELs were not negligible but ranged from 3% to 21% (Leisenring and Ryan, 1992). Finally, BMD methods provide a consistent framework for comparing the potency (severity of response at a given dose) of various substances and for extrapolating to doses associated with lower risks. As such, BMD methods may facilitate risk comparisons across an array of nanoscale and larger particles.

BMD methods require sufficient data to characterize the dose–response relationship. Dose–response relationships may show an increasing or decreasing trend depending on the endpoint (e.g., an increase in an adverse effect or a decrease in a normal function associated with increasing dose). At least two dose groups in addition to the control group are generally needed for BMD modeling, although a reasonable BMD estimate may be obtained if the elevated response in one of the exposed group is near the BMR (EPA, 2000). More dose groups may be needed to adequately describe highly nonlinear relationships. If adequate dose–response data are not available for BMD estimation, a NOAEL or LOAEL may be used as a point of departure (POD) for low-dose extrapolation (EPA, 2000). Toxicology study designs that take into consideration the BMD data requirements can greatly facilitate the study's utility for quantitative risk assessment.

3.1.4 Temporal Extrapolation

In an analysis by the US National Toxicology Program of LOAELs and NOAELs from 46 subacute, subchronic, and chronic studies of respiratory irritants acting mainly in the extrathoracic region, Kalberlah et al. (2002) estimated that the effect concentrations (e.g., LOAELs) in subchronic (13-week) underestimated the chronic response by a factor of approximately

7 (geometric mean) (2–21, 10th and 90th percentiles). The standard uncertainty factor of 10 to extrapolate from subchronic to chronic response (EPA, 2000) would thus seem to be reasonable on average, although it would not be sufficiently protective in some situations. In the current example for MWCNT, the adverse lung responses are assumed to relate to the total estimated lung dose (deposited or retained), which is the dose metric that has been associated with fibrotic and other adverse lung effects from exposure to various other types of poorly soluble particles in animals and humans (e.g., Dankovic et al., 2007; Kuempel et al., 2001a; Muhle et al., 1991). In this case, since the subchronic effect concentrations are converted to equivalent lung doses by accounting for duration of exposure, these estimates may better estimate the chronic effects than those reported by Kalberlah et al. (2002).

3.2 CASE STUDY EXAMPLE: CARBON NANOTUBES

Two recent subchronic inhalation studies in rats of MWCNT (Ma-Hock et al., 2009; Pauluhn, 2010a) provide examples of dose–response data currently available for quantitative risk assessment of some engineered nanomaterials. These studies are relevant to occupational risk assessment given that the target organ (lungs), exposure route (inhalation) and pattern (5 day/week, 6 h/day), and lung responses in the rats were similar to those observed in humans with occupational exposures to other poorly soluble respirable particles (Attfield and Seixas, 1995; Gardiner et al., 2001; Kuempel et al., 2001a).

3.2.1 Data Description

The two MWCNT subchronic studies in rats had similar study designs, although the MWCNT material varied somewhat in their physical–chemical properties. The MWCNT investigated in Ma-Hock et al. (2009) had a primary particle size of 5–15 nm in width and 1–10 μm in length and contained 9.6% Al_2O_3; the mass median aerodynamic diameter (MMAD) and geometric standard deviation (GSD) were approximately 1.2 and 2.7, respectively (median value reported). In the Pauluhn (2010a) study, the MWCNT had a primary particle size of ~10 nm in width and 200–1,000 nm in length and contained 0.5% Co; the MMAD and GSD were approximately 2.7 and 2.1, respectively (median value reported). In both studies, rats were exposed by inhalation 6 h/day, 5 day/week, for 13 weeks. Lung responses were examined at the end of the 13-week exposure in both studies; postexposure follow-up was up to 6 months in the Pauluhn (2010a) study.

The exposure concentrations in Ma-Hock et al. (2009) were 0, 0.1, 0.5, and 2.5 mg/m^3; a LOAEL of 0.1 mg/m^3 was identified for granulomatous inflammation, in which 30% of rats had developed a minimal or higher

grade based on histopathology. At 0.5 mg/m^3, 85% of the rats had developed lipoproteinosis. The exposure concentrations in Pauluhn (2010a) were 0, 0.1, 0.45, 1.62, and 5.98 mg/m^3. A NOAEL was identified at 0.1 mg/m^3 and the LOAEL was at 0.45 mg/m^3 for pulmonary inflammation, based on elevated polymorphonuclear leukocytes (PMNs) in bronchoalveolar lavage (BAL) fluid, and on alveolar interstitial (septal) thickening, of which 90% of rats had developed a minimal or higher grade based on histopathology (Pauluhn personal communication; Pauluhn, 2010a).

3.2.2 **Severity of Effects**

Quantitative risk assessment involves estimation of the severity and likelihood of an adverse response associated with exposure to a hazardous agent (NRC, 2009; Piegorsch and Bailer, 2005). Although pulmonary fibrosis has not been studied in CNT workers, it has been associated with occupational exposure to various types of respirable particles and fibers including carbon black (Gardiner et al., 2001), coal dust (Attfield and Seixas, 1995), silica (Park et al., 2002), and asbestos (Stayner et al., 2008). Chest radiograph or computerized tomography is used in medical examinations to identify the occurrence and severity of fibrosis. In animal studies, a more sensitive measure of pulmonary fibrosis is the amount of alveolar interstitial thickening. Since gas exchange occurs across the alveolar septal air/blood barrier, such thickening of the alveolar septum due to fibrosis can interfere with normal lung function.

The rat subchronic lung responses to inhaled MWCNT effects were relatively early stage (minimal or mild histopathology severity grades) for either pulmonary septal thickening including fibrosis (Pauluhn, 2010a) or granulomatous inflammation (Ma-Hock et al., 2009). In the Pauluhn (2010a) study, the alveolar septal thickening observed in response to CNT exposure persisted for at least 26 weeks after the end of the 13-week exposure (i.e., at week 39). Several toxicology studies in which mice were exposed to SWCNT or MWCNT by pharyngeal aspiration have also shown a dose-dependent alveolar septal thickening, and this response persisted or progressed with longer postexposure time (Mercer et al., 2008; Porter et al., 2010; Shvedova et al., 2005, 2008). Although limited information is available to evaluate whether the lung responses in animals exposed to CNT are associated with functional impairment, changes in breathing pattern in SWCNT-exposed mice have been noted (Shvedova et al., 2005). In addition, alveolar septal thickening has been considered relevant to humans and indicates "fundamental structural remodeling" (e.g., in response to ozone exposure) (EPA, 1996; Stockstill et al., 1995). In the

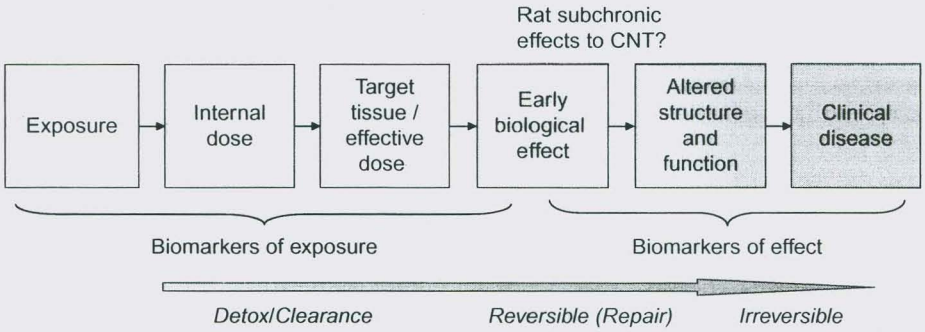

■ **FIGURE 3.1** Biological continuum from dose to disease , with consideration of the lung responses to CNT (carbon nanotubes) observed in the rat subchronic inhalation studies (Ma-Hock et al., 2009; Pauluhn, 2010a). *Source: Adapted from Schulte, P.A., 1989. A conceptual framework for the validation and use of biologic markers. Environ. Res. 48(2), 129–144.*

Ma-Hock et al. (2009) study, fibrosis was not evaluated; however, the findings of granulomatous inflammation and lipoproteinosis are consistent with the development of pulmonary fibrosis in rodents and humans (e.g., from silica exposure; Heppleston, 1975; Hoffmann et al., 1973; Porter et al., 2004). Therefore, these rat subchronic lung effects in response to CNT may be considered to be in the range of early biological responses associated with altered structure and function (Schulte, 1989; Figure 3.1).

A more detailed and quantitative scale of adverse effects has been developed for use in deriving inhalation reference concentrations (EPA, 1994). Based on that scale (from 0 to 10), these pulmonary changes observed in rats with subchronic exposure to MWCNT may correspond somewhere in the range of levels 6–8, although the observed effects may not align exactly with one level:

- Level 6 (LOAEL): Degenerative or necrotic tissue changes with no apparent decrement in organ function.
- Level 7 (LOAEL): Reversible slight changes in organ function.
- Level 8 (LOAEL/FEL (defined below): Pathological changes with definite organ dysfunction that are unlikely to be fully reversible.

These levels are consistent with the more qualitative evaluation depicted in Figure 3.1. Effect levels 6 and 7 are considered to be LOAELs, while level 8 is considered to be a LOAEL/FEL (EPA, 1994). A FEL is a "frank effect level," defined as an "exposure level that produces frankly apparent and unmistakable adverse effects, such as irreversible functional impairment or mortality, at a statistically and biologically significant increase in frequency or severity between an exposed population and its appropriate

control" (EPA, 1994). Clearly, a goal in risk assessment is to estimate levels of exposure that are not likely to be associated with any material impairment of health or functional capacity, even if exposures occur over a full working lifetime (OSH Act, 1970).

3.2.3 Risk Assessment Steps: Benchmark Dose Estimation

The steps in using rodent dose–response data of inhaled particles in occupational risk assessment, shown in Figure 3.2, are applied here to MWCNT. In the first step, the exposure–response data from the two published subchronic inhalation studies of MWCNT (Ma-Hock et al., 2009; Pauluhn, 2010a) are used because they provide data of relevance to workers (inhalation route of exposure, daily exposures), well-characterized materials (particle size data and chemical composition), and quantitative measures of dose and response. The rat lung responses of granulomatous inflammation (Ma-Hock et al., 2009) or pulmonary septal thickening (Pauluhn, 2010a) at minimal or higher severity (grade 1) based on histopathology are selected because they are sensitive, early-stage adverse lung responses to the CNT exposure, and are relevant to lung disease development in humans.

In the next step, a benchmark dose is estimated by fitting statistical models (using the BMD software, BMDS (EPA, 2000, 2010)) to rat dose–response data from each study (Ma-Hock et al., 2009; Pauluhn, 2010a). In this case, the "dose" is the airborne exposure concentration, resulting in the estimation of a benchmark concentration (BMC) (maximum likelihood estimate) and a lower 95% confidence limit estimate (BMC(L)). A challenge in using these data in risk assessment is that the multistage model was the only one in the BMD model suite (EPA, 2010) that converged to a unique solution, as well as provide an adequate fit to the data ($p > 0.1$ in a goodness of fit test) (EPA, 2000). This is due to the steep dose–response relationship and the sparse data near the 10% BMR, which provide little information for the curve fitting and resulted in multiple solutions in several models. Also, since the model optimization algorithm seeks the optimal fit to all the data, it is necessary to evaluate whether the 100% response groups influence the BMC(L) estimation. In such cases, the top dose group is typically dropped and the model refit (EPA, 2000). In either data set, this had little influence on the BMC(L) estimates (up to four decimal places) or the model fit (p-values remained adequate, i.e., $p > 0.1$ in goodness of fit test; EPA, 2000). The BMC(L) estimates, as shown in Tables 3.4 and 3.5) and Figures 3.3 and 3.4, are approximately 0.06 (0.02) mg/m^3 in Ma-Hock et al. (2009) and 0.1 (0.05) mg/m^3 in Pauluhn (2010a). These BMC(L) estimates are similar to or lower than the adverse effect levels in

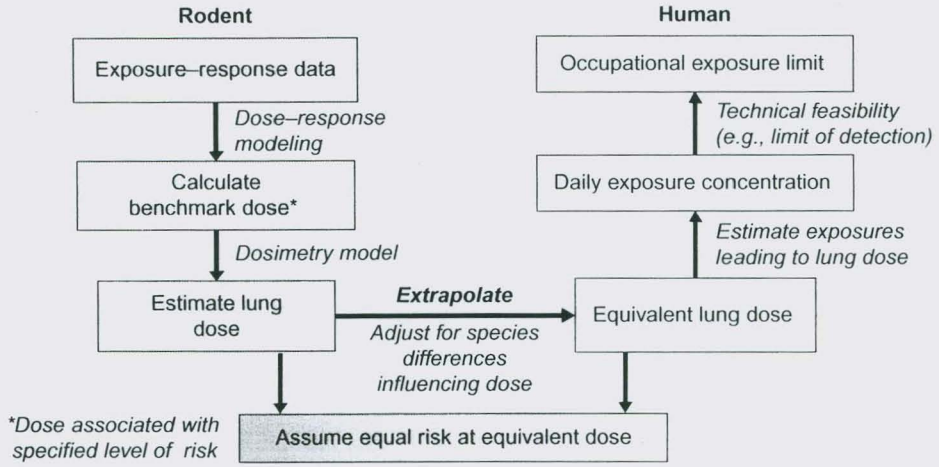

■ **FIGURE 3.2** Risk assessment steps using animal data of airborne particles, for example, carbon nanotubes, to develop occupational exposure limits.

Table 3.4 Benchmark Dose Estimates[a] and Associated Human Working Lifetime Airborne Concentrations – Based on Subchronic Inhalation of MWCNT in Rats and Estimated Deposited Lung Dose[b]

Rodent Study and Response[c]	Rat BMC(L)[d] (mg/m³)	Rat BMD(L)[e] (µg/lung)	Human-Equivalent BMD(L) (mg/lung)	Human-Equivalent BMC(L): 8-h TWA and 45 work-years (µg/m³)
Granulomatous inflammation (Ma-Hock et al., 2009)	0.060 (0.023)	21 (8.1)	5.4 (2.1)	0.51 (0.19)
Focal alveolar septal thickening (Pauluhn, 2010a)	0.10 (0.051)	28 (14)	7.2 (3.5)	0.77 (0.38)

[a] *Benchmark response level: 10% excess (added) risk in exposed animal (EPA, 2010).*
[b] *Estimated deposited lung dose in rats and humans estimated using MPPD 2.0 model (CIIT and RIVM, 2006); aerodynamic particle sizes (MMAD, GSD): 2.74 (2.11).*
[c] *Responses are histopathology severity grade 1 or higher.*
[d] *BMC(L)s: BMC, maximum likelihood estimate of the benchmark concentration; 95% LCL, 95% lower confidence limit of the BMC; dose–response data fit with multistage model (polynomial degree 2) (EPA, 2010). P-values for the rodent dose–response models: 0.99 for Ma-Hock et al. (2009) and 0.88 for Pauluhn (2010a) (deposited dose); 1.0 for Ma-Hock et al. (2009) and 0.93 for Pauluhn (2010a) (retained dose), respectively.*
[e] *BMD, estimated benchmark dose (maximum likelihood estimate); BMD(L), estimated 95% lower confidence limit of the BMD.*

those studies; that is, the LOAEL was 0.1 mg/m^3 in Ma-Hock et al. (2009); the LOAEL was 0.4 mg/m^3, and the NOAEL was 0.1 mg/m^3 in Pauluhn (2010a).

Next, the BMC(L) estimates are used to estimate an equivalent lung dose (deposited or retained) in rats. The amount of MWCNT deposited in the

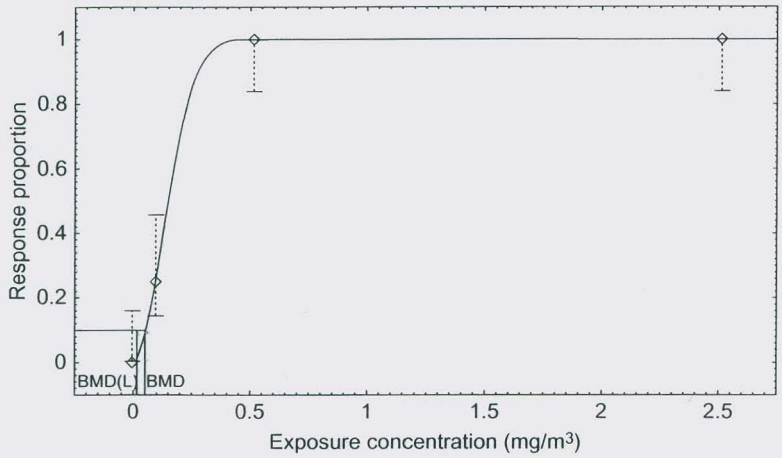

■ **FIGURE 3.3** Benchmark dose estimation: granulomatous inflammation (Ma-Hock et al., 2009). Multistage model, polynomial degree 2, $p = 0.99$. Rat subchronic BMC(L), 10% excess risk: 0.06 (0.02) mg/m^3. (*Note:* BMD is a general term for a benchmark dose (MLE estimate) and BMD(L) is the 95% lower confidence limit estimate of the BMD. In this chapter, the term BMD is used to refer to the lung dose, while the term BMC (benchmark concentration) refers to a BMD based on an airborne exposure concentration).

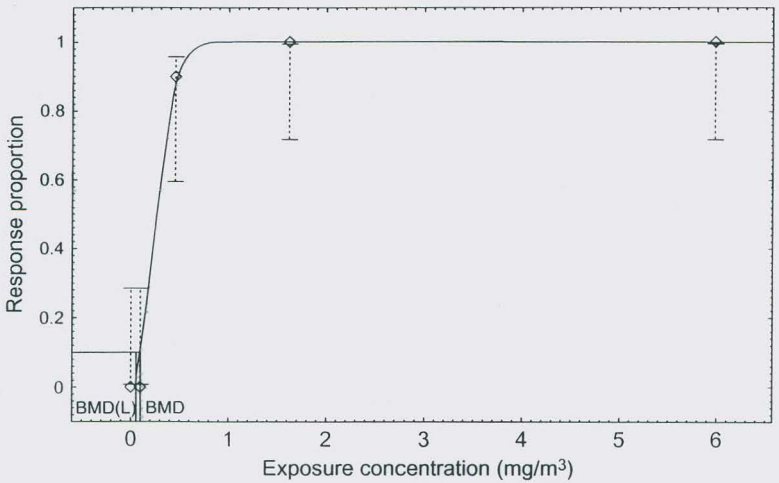

■ **FIGURE 3.4** Benchmark dose estimation: alveolar septal thickening (Pauluhn, 2010a). Multistage model, polynomial degree 2, $p = 0.88$. Rat subchronic BMD(L), 10% excess risk: 0.1 (0.05) mg/m^3. (*Note:* BMD is a general term for a benchmark dose (maximum likelihood estimate) and BMDL is the 95% lower confidence limit estimate of the BMD. In this chapter, the term BMD is used to refer to the lung dose, while the term BMC (benchmark concentration) refers to a BMD based on an airborne exposure concentration).

alveolar (or pulmonary) region of the rat lung at the end of the 13-week study (assuming no clearance) is calculated from data on the ventilation rate (which is related to body mass) (see Appendix), the exposure conditions, and the particle size-specific deposition fraction in the pulmonary region. In the following example, the BMC(L) from the Ma-Hock study (Figure 3.3; Table 3.4) is used:

$$\begin{aligned}\text{Deposited Dose} = {} & \text{Airborne concentration} \times \text{duration} \\ & \times \text{ventilation rate} \times \text{deposition fraction} \\ & \text{e.g., } 0.023\,\text{mg/m}^3 \times (6\,\text{hr/d} \times 5\,\text{d/wk} \times \\ & 13\,\text{wk}) \times 0.0126\,\text{m}^3\,\text{/hr} \times 0.072 \\ = {} & 0.0081\,\text{mg /rat lung}\end{aligned} \tag{3.2}$$

where the ventilation rate in the rat is calculated from: 0.21 L/min $\times$ 0.001 m^3/L $\times$ 60 min/h (see Appendix). The ventilation rate is based on species and body weight (EPA, 1994, 2006), assuming 300 g average body weight for male and female rats (since Ma-Hock et al. (2009) did not report the body weights, the values from Pauluhn (2010a) of approximately the same age and rat species/strain were used). The deposition fraction is estimated based on the MMAD and GSD in the rat multiple-path particle dosimetry (MPPD) model (CIIT and RIVM, 2006). Although the MPPD model has not been validated for CNT, using the measured aerodynamic diameter should provide a reasonable estimate of the deposition efficiency in the respiratory zone because aerodynamic diameter (which accounts for inertial behavior regardless of density and shape) accurately predicts the particle deposition efficiency in the respiratory tract regions (Hinds, 1999; Kulkarni et al., 2011). Deposited lung burden was used in this example as an estimate of the retained lung burden for CNT over the relatively short exposure period of the Ma-Hock et al. (2009) and Pauluhn (2010a) studies, because MWCNT clearance has been shown to be slower than predicted based on clearance data of other poorly soluble particles (Pauluhn, 2010a, 2010b).

The next step is to extrapolate the rat lung dose to a human-equivalent dose, by adjusting for species-specific differences in the surface area of the pulmonary (or gas exchange) region of the lungs. In making this extrapolation, it is assumed that rats and humans would have equal lung responses to an estimated equivalent dose per unit surface area of alveolar epithelial cells. The basis for this assumption is that the pulmonary region of the lungs (and specifically the alveolar epithelial cell surface) is the primary deposition target that results in interstitial fibrosis that has been observed

in both rodents and humans exposed to various types of airborne particles. Thus, the rat lung dose (0.0081 mg) is extrapolated to humans as follows:

$$\begin{aligned}\text{Human lung dose} &= \text{Rat lung dose} \times \text{Human/rat alveolar surface area} \\ &(102\,\text{m}^2/0.4\,\text{m}^2) = 2.1\,\text{mg in human lungs}\end{aligned} \tag{3.3}$$

where human and rat alveolar epithelial surface area are taken from morphometric analyses (Stone et al., 1992; Mercer et al., 1994).

Next is to estimate the workplace exposure scenario that would result in the human-equivalent lung dose. The estimated human 8-h time-weighted average (TWA) concentration over a 45-year working lifetime that would result in the human-equivalent lung dose in the pulmonary region of the lungs is calculated as:

$$\begin{aligned}&\frac{\text{Human-equivalent lung burden (mg)}}{|\text{Air intake} \times \text{exposure duration} \times \text{deposition fraction}|} \\ &= \frac{2.1\,\text{mg}}{|9.6(\text{m}^3/\text{d}) \times (5\,\text{d/wk} \times 50\,\text{wk/yr} \times 45\,\text{yr}) \times 0.099|} \\ &= 0.00019\,\text{mg/m}^3\end{aligned} \tag{3.4}$$

where the human-equivalent lung burden is from Eqn (3.3), the air intake is for the reference worker (ICRP, 1994) and the alveolar deposition fraction is based on the MMAD (GSD) as estimated in MPPD 2.0 (Yeh and Schum human deposition model) (CIIT and RIVM, 2006). As discussed above for the rat lung burden estimate, the aerodynamic diameter should provide a reasonable estimate of the deposited lung dose, while the retained lung dose estimates are more uncertain.

The benchmark dose and exposure concentration estimates shown in this example, based on deposited lung dose estimates (i.e., assuming no CNT clearance from the lungs), are shown in Table 3.4. In addition, Table 3.5 provides benchmark dose and exposure concentration estimates based on estimated retained lung dose in rats (at the end of 13 weeks) and equivalent retained dose estimates in humans (after 45-year working lifetime), assuming spherical particle deposition and clearance kinetics in MPPD 2.0 (CIIT and RIVM, 2006). The steps for deriving BMC(L) estimates based on retained lung dose are similar to those described above for deposited lung dose, except the MPPD model-based estimates of retained dose (which account for time-dependent clearance of the deposited dose) are used instead of the estimated deposited dose in Eqns (3.2) and (3.4). The human-equivalent BMC(L) estimates in Tables 3.4 and 3.5 indicate

Table 3.5 Benchmark Dose Estimates[a] and Associated Human Working Lifetime Airborne Concentrations – Based on Subchronic Inhalation of MWCNT in Rats and Estimated Retained Lung Dose[b]

Rodent Study and Response[c]	Rat BMC(L)[d] (mg/m^3)	Rat BMD(L)[e] (μg/lung)	Human-Equivalent BMD(L) (mg/lung)	Human-Equivalent BMC(L): 8-h TWA and 45 work-years ($\mu g/m^3$)
Granulomatous inflammation (Ma-Hock et al., 2009)	0.060 (0.023)	11 (3.8)	2.7 (0.97)	2.7 (1.0)
Focal alveolar septal thickening (Pauluhn, 2010a)	0.10 (0.051)	14 (6.5)	3.6 (1.7)	4.2 (1.9)

[a]Benchmark response level: 10% excess (added) risk in exposed animal (EPA, 2010).
[b]Retained lung doses in rats and humans estimated using MPPD 2.0 model (CIIT and RIVM, 2006); aerodynamic particle sizes (MMAD, GSD): 2.74 (2.11)
[c]Responses are histopathology severity grade 1 or higher.
[d]BMC(L)s: BMC, maximum likelihood estimate of the benchmark concentration; 95%LCL, 95% lower confidence limit of the BMC; dose–response data fit with multistage model (polynomial degree 2) (EPA, 2010). P-values for the rodent dose–response models: 1.0 for Ma-Hock et al. (2009) and 0.93 for Pauluhn (2010a), respectively.
[e]BMD, estimated benchmark dose (maximum likelihood estimate); BMD(L); estimated 95% lower confidence limit of the BMD.

that working lifetime exposures to 0.2–2 $\mu g/m^3$ (as 8-h TWA concentrations, lower 95% confidence limits; based on deposited or retained lung dose estimates) would be associated with a 10% excess risk of early-stage adverse lung effects (pulmonary inflammation and fibrosis) in workers. These airborne mass concentration estimates are quite low relative to estimates for other poorly soluble fine or ultrafine particles (e.g., Dankovic et al., 2007).

In order to perform risk characterization (step 4 of the risk assessment paradigm (NRC, 1983, 2009)), data are needed on the worker exposures. Because such data are limited (e.g., short-term or task-based area samples of airborne CNT concentration with few personal samples) (Bello et al., 2009; Johnson et al., 2010; Lee et al., 2010), it is not currently feasible to characterize the disease risk in workers producing or using CNT. However, these current studies indicate the potential for workplace airborne concentrations of concern and strongly support the need for extra precaution in controlling exposures to CNT (Schulte and Salamanca-Buentello, 2007).

The final step in the risk assessment process shown in Figure 3.2 is to develop an occupational exposure limit (OEL), which is beyond the scope of this chapter. Risk and nonrisk factors (e.g., technological feasibility of measuring and controlling exposures) are typically considered in the development of an OEL. These factors are also evaluated in conjunction with any

exposure measurement data to characterize the risk in a given population and to assess the need for additional protective measures such as personal protective equipment and medical monitoring.

3.3 DISCUSSION

Although the rat subchronic lung responses to MWCNT are early-stage (minimal or higher severity grade of granulomatous inflammation or alveolar septal thickening), a BMR is an effect level (e.g., 10%) that is considered biologically and statistically significant. In risk assessment practice, a human-equivalent BMD (i.e., the dose associated with the BMR) would not be used directly to develop an OEL. Instead, the BMD(L), or 95% lower confidence limit of the BMD, would typically be used as a point of departure (POD) to estimate doses associates with lower risk levels. Alternatively, a BMD(L) is treated like a NOAEL with the application of uncertainty factors (EPA, 2000).

A health-based OEL is based on an exposure associated with a low risk of disease over a full working lifetime. However, the technological feasibility of measuring or controlling exposures is also often considered in development of an OEL. For CNT (as for other materials) there are limitations in the technical feasibility of the method to measure airborne mass concentrations. For example, the limit of quantification (LOQ) of NIOSH method 5040 for elemental carbon including CNT is approximately 7 $\mu g/m^3$ as an 8-h TWA concentration (NIOSH, 2010). Thus, the risk estimates at this LOQ are greater than 10% for early-stage adverse lung effects (Section 3.2.3), which indicates the critical need to develop more sensitive measurement methods and to take additional precautionary measures (including engineering controls and personal protective equipment) when working with CNT that may become airborne and inhaled.

3.3.1 Comparison to Other Methods

In addition to the benchmark dose method illustrated here, it is relevant to compare these estimates (Tables 3.4 and 3.5) to those based on other methods. For example, if a NOAEL or LOAEL of 0.1 mg/m^3 (Ma-Hock et al., 2009; Pauluhn, 2010a, respectively) is used as the starting point, the human-equivalent working lifetime 8-h TWA concentration would be approximately 1 or 4 $\mu g/m^3$ based on the methods presented (using deposited or retained lung burden estimates), given that 0.1 mg/m^3 is also the BMC estimate based on the Pauluhn (2010a) study (Tables 3.4 and 3.5). Again, note that these are human-equivalent concentrations corresponding to 10% excess risk of early-stage adverse lung effects, and no uncertainty factors have been applied to these estimates.

A common method for extrapolating a NOAEL/LOAEL or BMD(L) estimate from animals to humans (e.g., to derive a chronic inhalation reference concentration or RfC) is the dosimetry adjustment factor (DAF) method for inhaled particles (EPA, 1994). In this method, the animal exposure concentration associated with an adverse effect (NOAEL, LOAEL, or BMC(L)) is adjusted for differences in the animal versus human exposure pattern (hours per day and days per week), then multiplied by the DAF. The DAF for inhaled particles is a series of ratios used to adjust for the interspecies differences that influence the deposited particle dose in the respiratory tract, including the animal versus human ventilation rate (V_E) (air volume inhaled per unit time); the animal versus human deposition fraction (DF) of particles in the relevant respiratory tract region(s); and a normalizing factor (NF) to adjust the deposited dose across species (e.g., the human vs. rat surface area of the respiratory tract region(s) is typically used for insoluble particles, which deposit and clear along the surface of the respiratory tract; EPA, 1994). Thus, a human-equivalent concentration would be calculated as: Effect concentration (animal) $\times$ [V_E(animal)/V_E(human)] $\times$ [DF(animal)/DF(human)] $\times$ [NF(human)/NF(animal)]. As seen here, many of the same adjustments are made as in the case study example (Section 3.2). However, the DAF method is based on an average concentration (i.e., the response is assumed to be related to the chronic average exposure concentration rather than to the cumulative dose as in Section 3.2). Appropriate uncertainty factors would be applied to the human-equivalent concentration in deriving an exposure limit (e.g., RfC; EPA, 1994).

In a recent risk assessment for MWCNT, Pauluhn (2010b) started with the NOAEL of 0.1 mg/m^3 from a rat subchronic inhalation study (Pauluhn, 2010a) to estimate a human-equivalent concentration as the basis for an OEL, by applying a series of interspecies adjustment factors (AFs) to the rat NOAEL. The first AF was to adjust for rat versus human differences in the ventilation rate, which Pauluhn (2010b) expressed per kg body weight: 0.14 (human)/0.29 (rat) = 0.5. These numbers were derived as follows: human reference worker breathing rate (8-h TWA) and weight: 9.6 m^3/70 kg (ICRP, 1994); and rat ventilation rate: 0.8 L/min per kg body weight $\times$ 360 min (in 6-h rat exposure day) $\times$ 0.001 m^3/L. The second AF was to adjust for interspecies differences in the percentage of MWCNT that is predicted to deposit in the pulmonary region in each species, based on an MMAD of 3 μm (Pauluhn, 2010b): 11.8% (human)/5.7% (rat) = 2. The third AF was a normalizing factor to adjust the deposited lung dose in each species based on the total alveolar macrophage (AM) cell volume, assuming a rat-based volumetric overload mode of action (also expressed per kg body weight), which resulted in an AF of 8.7 $\times$ 10^{10} (rat)/5.0 $\times$ 10^{11} (human) = 0.17

(Pauluhn, 2010b). The final AF was to normalize the retained lung dose based on an assumed constant factor of 10 × faster clearance in rats versus humans, based on first-order clearance kinetics. Combining these AFs, Pauluhn (2010b) derived an overall AF of: 0.5 × 2 × 0.17 × 10 = ~2. Dividing the rat NOAEL by this AF, a human-equivalent exposure concentration was calculated as 0.1 $mg/m^3/2 = 0.05\,mg/m^3$. No uncertainty factors were applied, and the human-equivalent concentration of $0.05\,mg/m^3$ was suggested as an OEL for MWCNT (Pauluhn, 2010b). (Note: the ratios used by Pauluhn (2010b) are inverse to those used in the DAF method described above (EPA, 1994); whereas EPA would multiply a NOAEL (or other effect level) by the DAF, Pauluhn (2010b) divided the NOAEL by the AF. Thus, caution is needed in applying these adjustment factor ratios).

Extrapolation of an animal effect level to estimate a human-equivalent concentration is of course influenced by the various factors and assumptions used, and reasonable alternatives may exist based on the scientific literature. For example, in the Pauluhn (2010b) approach, the expression of the rat and human ventilation rates per body weight has a large effect on the first AF. Since ventilation rates are already derived from a nonlinear allometric relationship to body weight (EPA, 1994, shown in the Appendix), typically these would not be adjusted again by body weight. If the whole animal or human ventilation rates are used instead, the first AF would be $9.6\,m^3$ per human 8-h workday/$0.085\,m^3$ per rat 6-h exposure day = 113 (vs. 0.5 in Pauluhn (2010b)). The rat ventilation rate of $0.085\,m^3$ is calculated for a 0.35-kg rat body weight (from equations in the Appendix) and is similar to an estimate of $0.1\,m^3$ based on the values reported in Pauluhn (2010b), that is, $0.29\,m^3$/6-h per kg × 0.35 kg rat = $0.1\,m^3$/6-h. Thus, the ventilation rates are similar, but are expressed differently in the AF, resulting in a quantitatively different AF. For the second AF, no alternative assumptions would seem reasonable since the pulmonary deposition percentages are based on the measured aerodynamic diameter of the particles; thus, the same human/rat pulmonary deposition AF of 2 is assumed here. For the third AF, an alternative assumption would be to adjust by the pulmonary surface area (Section 3.2.3; EPA, 1994) instead of using the alveolar macrophage cell volume to normalize the lung dose across species; this would result in an alternative AF of $0.4\,m^2$ (rat)/$102\,m^2$ (human) = 0.0039 (vs. 0.17 in Pauluhn (2010b)). Regarding the fourth AF, additional issues are discussed below, but for simplicity in this example, the same rat/human AF of 10 is assumed. Thus, using these alternative assumptions, the total AF would be 113 × 2 × 0.0039 × 10 = ~9. The alternative human-equivalent concentration would be 0.1 $mg/m^3/9 = 0.011\,mg/m^3$. This estimate is approximately five times lower than that of Pauluhn (2010b).

However, this is not a large difference given the uncertainty in the various extrapolation methods. Actually, these estimates are reasonably consistent as low airborne mass concentrations relative to larger size (fine) respirable particles or to other ultrafine (nanoscale) particles (e.g., Dankovic et al., 2007).

In the BMD example in Section 3.2, instead of using an AF of ~10 based on a simple first-order (one compartment) clearance model (as in Pauluhn (2010b)), the interspecies lung dose extrapolation was based on an estimate of the actual lung dose (deposited or retained) for a given exposure scenario. The ICRP (1994) human respiratory tract model (which is used in MPPD; CIIT and RIVM, 2006) includes three pulmonary clearance rate coefficients (three compartments) to estimate particle retention in the alveolar-interstitial region, including a fraction of the deposited dose that is cleared very slowly (approximately 10 year retention half-time). A simple one-compartment model assumed in Pauluhn (2010b) would underestimate the human retained lung burden (Kuempel and Tran, 2002). A higher-order long-term lung retention model that includes an interstitial-sequestration region (Kuempel et al., 2001b) has been shown to better fit several human data sets including high dust-exposed coal miners (Kuempel, 2000; Tran and Buchanan, 2000) and lower dose-exposed nuclear workers (Gregoratto et al., 2010). Revisions to the ICRP model including the alveolar-interstitial region based on the interstitial-sequestration model have been proposed (Bailey et al., 2008; Gregoratto et al., 2010). None of these models have been evaluated for CNT, however, and the animal data have shown that MWCNT clearance is slower for a given mass dose than that of spherical poorly soluble particles (Muller et al., 2005; Pauluhn, 2010a,b). Thus, the BMD examples, based on either the deposited or retained lung dose estimates (Tables 3.4 and 3.5), may represent the upper and lower bounds of the best estimate. That is, the deposited lung dose (assuming no CNT clearance) may overestimate the lung dose over time, whereas the retained lung dose (based on a poorly soluble spherical particle model) may underestimate the lung dose.

Despite these different approaches for dosimetric adjustment of a rodent adverse effect level (NOAEL or BMD) to estimate a human-equivalent dose, these various approaches all provide relatively low mass airborne exposure concentrations. By comparison, in a similar study design (13-week inhalation exposure) in rats exposed to ultrafine carbon black, the NOAEL was 1 mg/m^3 and the LOAEL for pulmonary inflammation and fibrosis was 7 mg/m^3 (Elder et al., 2005). Although dose spacing influences NOAEL and LOAEL values, these findings suggest that MWCNT are approximately 10 times more potent in causing pulmonary inflammation and fibrosis than ultrafine carbon black.

A recent update from the MPPD 2.0 to MPPD 2.1 (ARA, 2009) includes revised rat deposition efficiency prediction equations (Raabe et al., 1988), which result in increased predicted respirable particle deposition fractions in the head/extrathoracic region, and consequently lower predicted deposition fractions in the rat pulmonary region (Owen Price, ARA, personal communication). For the MWCNT particle sizes, this results in approximately half the estimated deposited dose of MWCNT in the rat pulmonary region (thus, the rat pulmonary deposition fraction reported by Pauluhn (2010b) would also be about half). The lower estimated dose associated with the same response proportion in the rat would result in lower rat BMD(L) and humans-equivalent BMC(L) estimates (by a factor of approximately two) than those shown in Tables 3.4 and 3.5. As additional data become available (e.g., in animal studies) to evaluate current lung dosimetry models for CNT, the uncertainties in CNT dose and risk estimation may be reduced.

3.3.2 **Research Needs**

Toxicological studies in animals and *in vitro* cell systems provide essential data for hazard and risk assessment of nanoparticles. Additional research needs for risk assessment of nanoparticles (which may also apply to risk assessment of other substances) include (1) determination of responses not only in the organ of initial exposure but also in distal organs; (2) identification of the nature of the hazard, including the severity of the effect and mechanism of action in animals and relevance to humans; (3) determination of a biologically effective dose metric that is associated with these adverse effects; and (4) generation of quantitative dose–response data in animal studies that are relevant to estimation of equivalent dose and disease in humans. In addition, toxicological studies can provide more specialized data that are needed to develop mechanistically based risk models, including (5) kinetic data on the dose to the target tissue over time to measure internal dose and develop dosimetry models; and (6) time course of the dose and response to develop biologically based models linking early biological responses and later disease outcomes. In addition, data on workplace exposures to nanomaterials are critically needed in order to characterize the risk and to take appropriate risk management measures to protect workers' health. Improvements in the sensitivity and specificity of measurement and analytical methods are needed for nanomaterials including CNT (NIOSH, 2010) in order to detect and quantify low mass concentrations. These low airborne mass concentrations are of concern based on the hazard data from the animal studies and the risk estimates derived from those data (e.g., case study example in this chapter).

3.3.3 Future Directions

Nanotechnology is capable of synthesizing nanoparticles of various sizes, shapes, dissolution rates, surface charge, hydrophobicity, surface functionalization, surface reactivity, chemistry, etc. Given the vast array of nanoparticles that are being developed, it will be necessary to develop strategies to more efficiently and effectively assess hazard and risk of nanoparticles to which workers may be exposed. The development of *in vitro* assays that can predict *in vivo* responses would facilitate initial hazard evaluation tests and screening to identify less hazardous nanomaterials (Rotroff et al., 2010). These assays require validation, although some promising studies are emerging. For example, the *in vitro* and *in vivo* dose–response relationships for inflammation-related responses have been shown to correlate well when dose is expressed as particle surface area and the reactivity of the surface is taken into account (Donaldson et al., 2008). More recently, *in vitro* cell assays of oxidative stress were shown to correlate well with *in vivo* rat acute lung responses based on the particle surface area dose of several spherical metal and metal oxide nanoparticles (Rushton et al., 2010). Development of a matrix of relationships between bioactivity and physical–chemical properties (i.e., quantitative structure activity relationships, QSAR) may also facilitate comparative potency and hazard ranking strategies.

Future advancements in risk assessment methods may include models to predict disease response based on early biological responses, such as cell signaling and gene expression data (Thomas et al., 2007, 2009). There is also a need to determine to what degree bolus exposures (intratracheal instillation or pharyngeal aspiration) of biopersistent nanoparticles, such as MWCNT, provide similar responses to an equivalent dose by inhalation. Preliminary data suggest that pharyngeal aspiration of a well-dispersed suspension of SWCNT results in a level of pulmonary inflammation and fibrosis that is similar to that seen after a 4-day inhalation resulting in the same lung burden of SWCNT (Mercer et al., 2008; Shvedova et al., 2008). In addition, a 1-day (6-h) inhalation exposure in rats showed a similar dose–response relationship for pulmonary septal thickening and fibrosis at 90 days postexposure (Ellinger-Ziegelbauer and Pauluhn, 2009) as the 13-week inhalation study (Pauluhn, 2010a) based on estimated deposited lung dose. Therefore, it appears that shorter-term exposure studies may provide data for comparison to the subchronic studies and expand the data base to evaluate the hazard of various types of CNT.

Chronic exposure studies are needed to evaluate the potential adverse effects that exhibit a long latency, such as lung cancer or mesothelioma.

Currently, some short-term studies of CNT have included positive controls, for example, crystalline silica, asbestos, ultrafine carbon black (Lam et al., 2004; Muller et al., 2005; Shvedova et al., 2005) for which chronic study data are available in animals and in epidemiology studies. These data provide a linkage between short-term effects in animals and chronic effects of relevance to humans. Such linkages provide opportunities for comparative potency analyses between these well-studied particles (a.k.a. reference or benchmark particles) and engineered nanoparticles, especially if information is available to indicate the same mode of action.

In the absence of complete information on the hazards and risks associated with exposure to nanomaterials, a higher level of precaution is needed in controlling exposures in the workplace. Animal studies indicate that inhaled nanoparticles, including CNT, may be more hazardous on an equal mass basis, than larger particles of the same chemical composition. Primary prevention through effective control of airborne exposure during production, use, or disposal of nanomaterials is essential to protect workers from developing occupational respiratory diseases.

ACKNOWLEDGEMENTS:

The authors would like to thank Dr. Ann Hubbs for her critical input concerning interpretation of the histopathology findings in the animal studies of CNT including those in the case study example. The authors would also like to thank Mr. Randall Smith for his statistical input regarding the BMD modeling of the animal dose–response data discussed in this chapter.

Disclaimer: The findings and conclusions in this Chapter are those of the authors and do not necessarily represent the view of the National Institute for Occupational Safety and Health.

3.4 APPENDIX: PULMONARY VENTILATION RATE CALCULATIONS

Species-specific average ventilation rates can be calculated based on the following allometric scaling equation:

$$\ln(V_E) = b_0 + b_1 \ln(\mathrm{BW}) \qquad (A.1)$$

where V_E is the minute ventilation (L/min); BW is body weight (kg); and b_0 and b_1 are the species-specific parameters; for the rat, b_0 and b_1 are –0.578 and 0.821, respectively (in Table 4.6 of EPA (1994)).

Minute ventilation (V_E) (L/min) is itself the product of the tidal volume (V_T) (L) and the breathing frequency (f) (min) (EPA, 1994):

$$V_E = V_T \times f \tag{A.2}$$

3.4.1 Rat Ventilation Rate

The default values for minute ventilation in the MPPD 2.0 rat model (CIIT and RIVM, 2006) is 0.21 L/min, based on the default values of 2.1 ml (V_T) and 102/min (f):

$$0.21(\text{L/min}) = 2.1(\text{ml}) \times 102(/\text{min}) \times (1/1000)(\text{L/ml}) \tag{A.3}$$

This minute ventilation corresponds to a 300-g rat, based on Eqn (A.1):

$$0.21\text{L/min} = \text{Exp}\,[-0.578 + 0.821 \times \ln(0.3)] \tag{A.4}$$

Minute ventilation values for the rats in the subchronic inhalation studies (Ma-Hock et al., 2009; Pauluhn, 2010a) were also calculated based on body weight. Pauluhn (2010a) reported male and female rat body weights of 369 and 245 g, respectively, in the control (unexposed) group at 13 weeks. Since the alveolar septal thickening response data were reported for 10 male rats per dose group, the male rat body weight (and calculated minute ventilation) was used to estimate deposited and retained lung dose in the Pauluhn study (2010a). Ma-Hock et al. (2009) did not report the rat body weight, although the rat strain (Wistar) and study duration (13 weeks) were the same as in Pauluhn (2010a). Since the granulomatous inflammation response data in Ma-Hock et al. (2009) were combined for the 10 male and 10 female rats in each dose group (because response proportions were statistically consistent), an average rat body weight in male and female rats of 300 g was assumed, based on the 300 g rat body weight used in the default minute ventilation in MPPD 2.0 (CIIT and RIVM, 2006) and the male and female average body weight of 307 g reported in Pauluhn (2010a).

Thus, based on Eqn (A.1), a minute ventilation of 0 0.21 L/min is calculated for female and male rats in Ma-Hock et al. (2009) (same as MPPD 2.0 default) and 0.25 L/min for male rats in Pauluhn (2010a). Assuming the same breathing frequency (102/min), a tidal volume of 2.45 ml is calculated (Eqn (A.3)) and used instead of the default value in MPPD 2.0 (CIIT and RIVM, 2006) in estimating the rat lung dose in the Pauluhn (2010a) data.

3.4.2 Human Ventilation Rate

In the human MPPD 2.0 model (CIIT and RIVM, 2006), the default pulmonary ventilation rate is 7.5 L/min, based on default values of 12/min

breathing frequency and 625 ml tidal volume. The "reference worker" ventilation rate is 20 L/min (ICRP, 1994) or 9.6 m^3/8-h (given 0.001 m^3/L and 480 min/8-h). In these estimates, 17.5/min breathing frequency and 1143 ml tidal volume were used in MPPD 2.0 to correspond to a 20-L/min reference worker ventilation rate.

REFERENCES

ARA, 2009. Multiple-Path Particle Deposition (MPPD 2.1): A Model for Human and Rat Airway Particle Dosimetry. Applied Research Associates, Inc, Raleigh, NC.

Asakura, M., Sasaki, T., Sugiyama, T., Takaya, M., Koda, S., Nagano, K., et al., 2010. Genotoxicity and cytotoxicity of multi-wall carbon nanotubes in cultured Chinese hamster lung cells in comparison with chrysotile A fibers. J. Occup. Health 52 (3), 155–166.

Attfield, M.D., Seixas, N.S., 1995. Prevalence of pneumoconiosis and its relationship to dust exposure in a cohort of U.S. bituminous coal miners and ex-miners. Am. J. Ind. Med. 27 (1), 137–151.

Baan, R.A., 2007. Carcinogenic hazards from inhaled carbon black, titanium dioxide, and talc not containing asbestos or asbestiform fibers: recent evaluations by an IARC Monographs Working Group. Inhal. Toxicol. 19 (Suppl. 1), 213–228.

Bailey, M., Ansoborlo, E., Etherington, G., Gregoratto, D., Guilmette, R., Marsh, J., et al., 2008. Proposed updating of the ICRP human respiratory tract model. In: Proc. 12th International Congress of the International Radiation Protection Association, Buenos Aires, October 19–24, 2008. http://www.irpa12.org.ar/fullpapers/FP0947.pdf.

Bellmann, B., Muhle, H., Creutzenberg, O., Dasenbrock, C., Kilpper, R., MacKenzie, J.C., et al., 1991. Lung clearance and retention of toner, utilizing a tracer technique, during chronic inhalation exposure in rats. Fundam. Appl. Toxicolo. 17 (2), 300–313.

Bello, D., Wardle, B.L., Yamamoto, N., deVillora, R.G., Garcia, E.J., Hart, A.J., et al., 2009. Exposure to nanoscale particles and fibers during machining of hybrid advanced composites containing carbon nanotubes. J. Nanopart. Res. 11 (1), 231–249.

Bermudez, E., Mangum, J.B., Asgharian, B., Wong, B.A., Reverdy, E.E., Janszen, D.B., et al., 2002. Long-term pulmonary responses of three laboratory rodent species to subchronic inhalation of pigmentary titanium dioxide particles. Toxicol. Sci. 70 (1), 86–97.

Bermudez, E., Mangum, J.B., Wong, B.A., Asgharian, B., Hext, P.M., Warheit, D.B., et al., 2004. Pulmonary responses of mice, rats, and hamsters to subchronic inhalation of ultrafine titanium dioxide particles. Toxicol. Sci. 77, 347–357.

Castranova, V., 1998. Particulates and the airways: basic biological mechanisms of pulmonary pathogenicity. Appl. Occup. Environ. Hyg. 13 (8), 613–616.

Castranova, V., 2000. From coal mine dust to quartz: mechanisms of pulmonary pathogenicity. Inhal. Toxicol. 3, 7–14.

CIIT and RIVM, 2006. Multiple Path Particle Dosimetry (MPPD, version 2.0): A Model for Human and Rat Airway Particle Dosimetry. Centers for Health Research (CIIT): Research Triangle Park, NC.

Crump, K.S., 1984. A new method for determining allowable daily intakes. Fundam. Appl. Toxicol. 4, 854–871.

Crump, K.S., 1995. Calculation of benchmark doses from continuous data. Fundam. Appl. Toxicol. 15 (1), 79–89.

Crump, K.S., 2002. Critical issues in benchmark calculations from continuous data. Crit. Rev. Toxicol. 32 (3), 133–153.

Dankovic, D., Kuempel, E., Wheeler, M., 2007. An approach to risk assessment for TiO_2. Inhal. Toxicol. 19 (Suppl 1), 205–212.

Donaldson, K., Beswick, P.H., Gilmour, P.S., 1996. Free radical activity associated with the surface of particles: a unifying factor in determining biological activity? Toxicol. Lett. 88, 293–298.

Donaldson, K., Borm, P.J., Oberdörster, G., Pinkerton, K.E., Stone, V., Tran, C.L., 2008. Concordance between in vitro and in vivo dosimetry in the proinflammatory effects of low-toxicity, low-solubility particles: the key role of the proximal alveolar region. Inhal. Toxicol. 20 (1), 53–62.

Driscoll, K.E., 1996. Role of inflammation in the development of rat lung tumors in response to chronic particle exposure. In: Mauderly, J.L., McCunney, R.J. (Eds.), Particle Overload in the Rat Lung and Lung Cancer, Implications for Human Risk Assessment (pp. 139–153). Taylor and Francis, Washington, DC.

Elder, A., Gelein, R., Finkelstein, J.N., Driscoll, K.E., Harkema, J., Oberdörster, G., 2005. Effects of subchronically inhaled carbon black in three species. I. Retention kinetics, lung inflammation, and histopathology. Toxicol. Sci. 88 (2), 614–629.

Elder, A., Gelein, R., Silva, V., Feikert, T., Opanashuk, L., Carter, J., et al., 2006. Translocation of inhaled ultrafine manganese oxide particles to the central nervous system. Environ. Health Perspect. 114, 1172–1178.

Ellinger-Ziegelbauer, H., Pauluhn, J., 2009. Pulmonary toxicity of multi-walled carbon nanotubes (Baytubes®) relative to quartz following a single 6 h inhalation exposure of rats and a 3 months post-exposure period. Toxicology 266, 16–29.

EPA, 1994. Methods for Derivation of Inhalation Reference Concentrations and Application of Inhalation Dosimetry. U.S. Environmental Protection Agency, Research Triangle Park, NC. EPA/600/8-90/066F, October 1994, pp. 4–26 thru 4–28.

EPA, 1996. Air Quality Criteria for Ozone and Related Photochemical Oxidants. Office of Research and Development, National Center for Environmental Assessment, U.S. Environmental Protection Agency, Washington, DC. EPA/600/P-93/004aF. vol. III, chapter 8, p78.

EPA, 2000. Benchmark Dose Technical Guidance Document. Risk Assessment Forum, U.S. Environmental Protection Agency, Washington, D.C. External review draft. EPA/630/R-00/001.

EPA, 2006. Approaches for the Application of Physiologically Based Pharmacokinetic (PBPK) Models and Supporting Data in Risk Assessment. National Center for Environmental Assessment, Office of Research and Development, U.S. Environmental Protection Agency, Washington, D.C.

EPA, 2010. Benchmark Dose Software. U.S. Environmental Protection Agency, National Center for Environmental Assessment, Washington, D.C. Version 2.1.2

Gardiner, K., van Tongeren, M., Harrington, M., 2001. Respiratory health effects from exposure to carbon black: results of the phase 2 and 3 cross sectional studies in the European carbon black manufacturing industry. Occup. Environ. Med. 58, 496–503.

Geiser, M., Rothen-Rutishauser, B., Kapp, N., Schurch, S., Kreyling, W., Schulz, H., et al., 2005. Ultrafine particles cross cellular membranes by nonphagocytic

mechanisms in lungs and in cultured cells. Environ. Health Perspect. 113 (11), 1555–1560.

Gregoratto, D., Bailey, M.R., Marsh, J.W., 2010. Modelling particle retention in the alveolar-interstitial region of the human lungs. J. Radiol. Prot. 30 (3), 491–512.

Grubek-Jaworskaa, H., Nejmana, P., Czumiska, K., Przybyłowskia, T., Huczkoc, A., Langec, H., et al., 2006. Preliminary results on the pathogenic effects of intratracheal exposure to one-dimensional nanocarbons. Carbon 44 (6), 1057–1063.

Heppleston, A.G., 1975. Animal model of human disease. Pulmonary alveolar lipoproteinosis. Animal model: Silica-induced pulmonary alveolar lipo-proteinosis. Am. J. Pathol. 78 (1), 171–174.

Hinds, W.C., 1999. Respiratory deposition. In: Hinds, W.C. (Ed.), Aerosol Technology: Properties, Behavior, and Measurement of Airborne Particles (second ed.). J. Wiley and Sons, New York Chapter 11.

Hoffmann, E.O., Laberty, J., Pizzolato, P., Coover, J., 1973. The ultrastructure of acute silicosis. Arch. Pathol. 96, 104–107.

ICRP, 1994. Human respiratory tract model for radiological protection. In: Smith, H. (Ed.), Annals of the ICRP. International Commission on Radiological Protection, ICRP Publication No. 66, Tarrytown, New York.

ILSI (International Life Sciences Institute), The relevance of the rat lung response to particle overload for human risk assessment: a workshop consensus report. Inhal. Toxicol. 12, 1–17.

Johnson, D.R., Methner, M.M., Kennedy, A.J., Stevens, J.A., 2010. Potential for occupational exposure to engineered carbon-based nanomaterials in environmental laboratory studies. Environ. Health Perspect. 118 (1), 49–54.

Kalberlah, F., Föst, U., Schneider, K., 2002. Time extrapolation and interspecies extrapolation for locally acting substances in case of limited toxicological data. Ann. Occup. Hyg. 46 (2), 175–185.

Kuempel, E.D., 2000. Comparison of human and rodent lung dosimetry models for particle clearance and retention. Drug Chem. Toxicol. 23 (1), 203–222.

Kuempel, E.D., Tran, C.L., Bailer, A.J., Porter, D.W., Hubbs, A.F., Castranova, V., 2001a. Biological and statistical approaches to predicting human lung cancer risk from silica. J. Environ. Pathol. Toxicol. Oncol. 20 (Suppl 1), 15–32.

Kuempel, E.D., O'Flaherty, E.J., Stayner, L.T., Smith, R.J., Green, F.H.Y., Vallyathan, V., 2001b. A biomathematical model of particle clearance and retention in the lungs of coal miners. Part I. Model development. Regul. Toxicol. Pharmacol. 34, 69–87.

Kuempel, E.D., Tran, C.L., 2002. Comparison of human lung dosimetry models: implications for risk assessment. Ann. Occup. Hyg. 46 (Suppl. 1), 337–341.

Kuempel, E.D., Tran, C.L., Castranova, V., Bailer, A.J., 2006. Lung dosimetry and risk assessment of nanoparticles: evaluating and extending current models in rats and humans. Inhal. Toxicol. 18 (10), 717–724.

Kulkarni, P., Sorensen, C.M., Baron, P.A., Harper, M., 2011. Nonspherical particle measurements: shape factor, fractals, and fibers. In: Kulkarni, P., Baron, P., Willeke, K. (Eds.), Aerosol Measurement: Principles, Techniques, and Applications. John Wiley and Sons, New York, NY.

Lam, C.W., James, J.T., McCluskey, R., Hunter, R.L., 2004. Pulmonary toxicity of single-wall carbon nanotubes in mice 7 and 90 days after intratracheal instillation. Toxicol. Sci. 77 (1), 126–134.

Lee, J.H., Lee, S.B., Bae, G.N., Jeon, K.S., Yoon, J.U., Ji, J.H., et al., 2010. Exposure assessment of carbon nanotube manufacturing workplaces. Inhal. Toxicol. 22 (5), 369–381.

Leisenring, W., Ryan, L., 1992. Statistical properties of the NOAEL. Regul. Toxicol. Pharmacol. 15 (2 Pt 1), 161–171.

Li, N., Sioutas, C., Cho, A., Schmitz, D., Misra, C., Sempf, J., et al., 2003. Ultrafine particulate pollutants induce oxidative stress and mitochondrial damage. Environ. Health Perspect. 111 (4), 455–460.

Li, Z., Hulderman, T., Salmen, R., Chapman, R., Leonard, S.S., Young, S-H., et al., 2007. Cardiovascular Effects of Pulmonary Exposure to Single-Wall Carbon Nanotubes. Environ. Health Perspect. 115, 377–382.

Ma-Hock, L., Treumann, S., Strauss, V., Brill, S., Luizi, F., Mertler, M., et al., 2009. Inhalation toxicity of multi-wall carbon nanotubes in rats exposed for 3 months. Toxicol. Sci. 112 (2), 468–481.

Mangum, J.B., Turpin, E.A., Antao- Menezes, A., Cesta, M.F., Bermudez, E., Bonner, J.C., 2006. Single-walled carbon nanotube (SWCNT)-induced interstitial fibrosis in the lungs of rats is associated with increased levels of PDGF mRNA and the formation of unique intercellular carbon structures that bridge alveolar macrophages in situ. Part. Fibre. Toxicol. 3 (15).

Mercer, R.R., Hubbs, A.F., Scabilloni, J.F., Wang, L., Batelli, L.A., Schwegler-Berry, D., et al., 2010. Distribution and persistence of pleural penetrations by multi-walled carbon nanotubes. Part. Fibre Toxicol. 7, 28.

Mercer, R.R., Russell, M.L., Roggli, V.L., Crapo, J.D., 1994. Cell number and distribution in human and rat airways. Am. J. Respir. Cell Mol. Biol. 10, 613–624.

Mercer, R., Scabilloni, J., Wang, L., Kisin, E., Murray, A.D., Shvedova, A.A., et al., 2008. Alteration of deposition patterns and pulmonary response as a result of improved dispersion of aspirated single-walled carbon nanotubes in a mouse model. Am. J. Physiol. Lung. Cell. Mol. Physiol. 294, L87–L97.

Muhle, H., Bellmann, B., Creutzenberg, O., Dasenbrock, C., Ernst, H., Kilpper, R., et al., 1991. Pulmonary response to toner upon chronic inhalation exposure in rats. Fundam. Appl. Toxicol. 17, 280–299.

Muller, J., Delos, M., Panin, N., Rabolli, V., Huaux, F., Lison, D., 2009. Absence of carcinogenic response to multiwall carbon nanotubes in 2-year bioassay in the peritoneal cavity of the rat. Toxicol. Sci. 110 (2), 442–448.

Muller, J., Huaux, F., Fonseca, A., Nagy, J.B., Moreau, N., Delos, M., 2008. Structural defects play a major role in the acute lung toxicity of multiwall carbon nanotubes: toxicological aspects. Chem. Res. Toxicol. 21, 1698–1705.

Muller, J., Huaux, F., Moreau, N., Misson, P., Heilier, J.F., Delos, M., et al., 2005. Respiratory toxicity of multi-wall carbon nanotubes. Toxicol. Appl. Pharmacol. 207 (3), 221–231.

NIOSH, 2010. Current Intelligence Bulletin Occupational Exposure to Carbon Nanotubes and Nanofibers. Draft for Public Comment, November 2010. Department of Health and Human Services, Centers for Disease Control and Prevention, National Institute for Occupational Saftety and Health. http://www.cdc.gov.niosh/docket/review/docket161A/.

NRC, 1993. Risk Assessment in the Federal Government: Managing the Process. National Academy Press, Washington, D.C.. Committee on the Institutional Means

for Assessment of Risks to Public Health, Commission on Life Sciences, National Research Council.

NRC, 2009. Science and Decisions: Advancing Risk Assessment. Committee on Improving Risk Analysis Approaches Used by the U.S. EPA, Board on Environmental Studies and Toxicology, Division on Earth and Life Studies, National Research Council of the National Academies. The National Academies Press, Washington, DC ISBN-10: 0-309-12046-2.

Oberdörster, G., Ferin, J., 1992. Metal compounds used in new technologies: metal oxides of ultrafine particles have increased pulmonary toxicity. Merian, E., Haerdi, W. Metal Compounds in Environment and Life, vol. 4. Science and Technology Letters, Middlesex, UK.

Oberdörster, G., Elder, A., Rinderknecht, A, 2009. Nanoparticles and the brain: cause for concern? J. Nanosci. Nanotechnol. 9 (8), 4996–5007.

Oberdörster, G., Ferin, J., Morrow, P.E., 1992. Volumetric loading of alveolar macrophages (AM): a possible basis for diminished AM-mediated particle clearance. *Experimental Lung*. Research 18 (1), 87–104.

Oberdörster, G., Oberdörster, E., Oberdörster, J., 2005. Nanotoxicology: an emerging discipline evolving from studies of ultrafine particles. Environ. Health Perspect. 113 (7), 823–839.

Oberdörster, G., Sharp, Z., Atudorei, V., Elder, A., Gelein, R., Lunts, A., et al., 2002. Extrapulmonary translocation of ultrafine carbon particles following whole-body inhalation exposure of rats. J. Toxicol. Environ. Health A 65, 1531–1543.

Oberdörster, G., Yu, C.P., 1990. The carcinogenic potential of inhaled diesel exhaust: a particle effect? J. Aerosol Sci. 21 (Suppl 1), S397–S401.

OSH Act, 1970. Occupational Safety and Health Act of 1970. Public Law 91-596, 84 STAT. 1590, 91st Congress, S.2193, December 29, 1970, as amended through January 1, 2004.

Park, R., Rice, F., Stayner, L., Smith, R., Gilbert, S., Checkoway, H., 2002. Exposure to crystalline silica, silicosis, and lung disease other than cancer in diatomaceous earth industry workers: a quantitative risk assessment. Occup. Environ. Med. 59 (1), 36–43.

Pauluhn, J., 2010a. Subchronic 13-week inhalation exposure of rats to multiwalled carbon nanotubes: toxic effects are determined by density of agglomerate structures, not fibrillar structures. Toxicol. Sci. 113 (1), 226–242.

Pauluhn, J., 2010b. Multi-walled carbon nanotubes (Baytubes): approach for derivation of occupational exposure limit. Regul. Toxicol. Pharmacol. 57 (1), 78–89.

Piegorsch, W.W., Bailer, A.F., 2005. Quantitative risk assessment with stimulus-response data Analyzing Environmental Data. John Wiley & Sons, Ltd, Chichester, West Sussex, England. Chapter 4.

Poland, C.A., Duffin, R., Kinloch, I., Maynard, A., Wallace, W.A., Seaton, A., 2008. Carbon nanotubes introduced into the abdominal cavity of mice show asbestos-like pathogenicity in a pilot study. Nat. Nanotechnol. 3 (7), 423–428.

Porter, D.W., Hubbs, A.F., Mercer, R., Robinson, V.A., Rasey, D., McLaurin, J., et al., 2004. Progresssion of lung inflammation and damage in rats after cessation of silica inhalation. Toxicol. Sci. 79, 370–380.

Porter, D.W., Hubbs, A.F., Mercer, R.R., Wu, N., Wolfarth, M.G., Sriram, K., et al., 2010. Mouse pulmonary dose-and time course-responses induced by exposure to multi-walled carbon nanotubes. Toxicology 269, 136–147.

Raabe, O.G., Al-Bayati, M.A., Teague, S.V., Rasolt, A., 1988. Regional deposition of inhaled monodisperse coarse and fine aerosol particles in small laboratory animals. Ann. Occup. Hyg. 32 (suppl.), 53–63.

Reddy, A.R., Krishna, D.R., Reddy, Y.N., Himabindu, V., 2010. Translocation and extra pulmonary toxicities of multi wall carbon nanotubes in rats. Toxicol. Mech. Method 20 (5), 267–272.

Rotroff, D.M., Wetmore, B.A., Dix, D.J., Ferguson, S.S., Clewell, H.J., Houck, K.A., et al., 2010. Incorporating human dosimetry and exposure into high-throughput in vitro toxicity screening. Toxicol. Sci. 117 (2), 348–358.

Rushton, E.K., Jiang, J., Leonard, S.S., Eberly, S., Castranova, V., Biswas, P., et al., 2010. Concept of assessing nanoparticle hazards considering nanoparticle dosemetric and chemical/biological response metrics. J. Toxicol. Environ. Health A 73 (5), 445–461.

Sager, T.M., Castranova, V., 2009. Surface area of particle administered versus mass in determining the pulmonary toxicity of ultrafine and fine carbon black: comparison to ultrafine titanium dioxide. Part. Fibre Toxicol. 6, 15.

Sager, T.M., Kommineni, C., Castranova, V., 2008. Pulmonary response to intratracheal instillation of ultrafine versus fine titanium dioxide: role of particle surface area. Part. Fibre Toxicol. 5, 17.

Sargent, L.M., Shvedova, A.A., Hubbs, A.F., Salisbury, J.L., Benkovic, S.A., Kashon, M.L., et al., 2009. Induction of aneuploidy by single-walled carbon nanotubes. Environ. Mol. Mutagen. 50 (8), 708–717.

Sargent, L.M., Reynolds, S.H., Hubbs, A.F., Benkovic, S.A., Lowry, D.T., Kashon, M.L., et al., 2011. Understanding carbon nanotube genotoxicity. The Toxicologist 120, A59.

Schins, R.P.F., Knaapen, A.M., 2007. Genotoxicity of poorly soluble particles. Inhal. Toxicol. 19 (Suppl. 1), 189–198.

Schulte, P.A., 1989. A conceptual framework for the validation and use of biologic markers. Environ. Res. 48 (2), 129–144.

Schulte, P.A., Salamanca-Buentello, F., 2007. Ethical and scientific issues of nanotechnology in the workplace. Environ. Health Perspect. 115, 5–12.

Semmler, M., Seitz, J., Erbe, F., Mayer, P., Heyder, J., Oberdörster, G., et al., 2004. Long-term clearance kinetics of inhaled ultrafine insoluble iridium particles from the rat lung, including transient translocation into secondary organs. Inhal. Toxicol. 16 (6–7), 453–459.

Semmler-Behnke, M., Takenaka, S., Fertsch, S., Wenk, A., Seitz, J., Mayer, P., et al., 2007. Efficient elimination of inhaled nanoparticles from the alveolar region: evidence for interstitial uptake and subsequent reentrainment onto airways epithelium. Environ. Health Perspect. 115 (5), 728–733.

Shvedova, A.A., Kisin, E.R., Mercer, R., Murray, A.R., Johnson, V.J., Potapovich, A.I., et al., 2005. Unusual inflammatory and fibrogenic pulmonary responses to single-walled carbon nanotubes in mice. Am. J. Physiol. Lung Cell. Mol. Physiol. 289, L698–L708.

Shvedova, A.A., Kisin, E., Murray, A.R., Johnson, V.J., Gorelik, O., Arepalli, S., et al., 2008. Inhalation versus aspiration of single walled carbon nanotubes in C57BL/6 mice: inflammation, fibrosis, oxidative stress and mutagenesis. Am. J. Physiol. Lung Cell. Mol. Physiol. 295, L552–L565.

Stayner, L., Kuempel, E., Gilbert, S., Hein, M., Dement, J., 2008. An epidemiological study of the role of chrysotile asbestos fibre dimensions in determining respiratory disease risk in exposed workers. Occup. Environ. Med. 65 (9), 613–619.

Stockstill, B.L., Chang, L.Y., Ménache, M.G., Mellick, P.W., Mercer, R.R., Crapo, J.D., 1995. Bronchiolarized metaplasia and interstitial fibrosis in rat lungs chronically exposed to high ambient levels of ozone. Toxicol. Appl. Pharmacol. 134 (2), 251–263.

Stone, K.C., Mercer, R.R., Gehr, P., Stockstill, B., Crapo, J.D., 1992. Allometric relationships of cell numbers and size in mammalian lung. Am. J. Respir. Cell Mol. Biol. 6, 235–243.

Takagi, A., Hirose, A., Nishimura, T., Fukumori, N., Ogata, A., Ohashi, N., 2008. Induction of mesothelioma in p53+/– mouse by intraperitoneal application of multi-wall carbon nanotube. J. Toxicol. Sci. 33 (1), 105–116.

Takenaka, S., Karg, E., Roth, C., Schulz, H., Ziesenis, A., Heinzmann, U., et al., 2001. Pulmonary and systemic distribution of inhaled ultrafine silver particles in rats. Environ. Health Perspect. 109 (Suppl 4), 547–551.

Thomas, R.S., Bao, W., Chu, T.M., Bessarabova, M., Nikolskaya, T., Nikolsky, Y., et al., 2009. Use of short-term transcriptional profiles to assess the long-term cancer-related safety of environmental and industrial chemicals. Toxicol. Sci. 112 (2), 311–321.

Tran, C.L., Buchanan, D., 2000. Development of a Biomathematical Lung Model to Describe the Exposure-Dose Relationship for Inhaled Dust among U.K. Coal Miners. Institute of Occupational Medicine, Edinburgh, UK. IOM Research Report TM/00/02.

U.S. Supreme Court, 1980. Industrial Union Department, AFL-CIO v. American Petroleum Institute et al., Case Nos. 78–911, 78–1036. Supreme Court Reporter 100, 2844–2905.

Wang, L., Mercer, R.R., Rojanasakul, Y.A., Lu, Y., Scabilloni, J.F., et al., 2010. Direct fibrogenic effects of dispersed single-walled carbon nanotubes on human lung fibroblasts. J. Toxicol. environ. Health. Part A. 73(5), 410–422.

White, R.H., Cote, I., Zeise, L., Fox, M., Dominici, F., Burke, T.A., et al., 2009. State-of-the-science workshop report: issues and approaches in low-dose-response extrapolation for environmental health risk assessment. Environ. Health Perspect. 117 (2), 283–287.

Assessing Nanoparticle Risks to Human Health

Edited by Gurumurthy Ramachandran

ELSEVIER

AMSTERDAM • BOSTON • HEIDELBERG • LONDON
NEW YORK • OXFORD • PARIS • SAN DIEGO
SAN FRANCISCO • SINGAPORE • SYDNEY • TOKYO
William Andrew is an imprint of Elsevier

Micro & Nano Technologies Series

Published Titles

9780815515739	Francois Leonard	*Physics of Carbon Nanotube Devices* (2009)
9780815515784	Mamadou Diallo, Jeremiah Duncan, Nora Savage, Anita Street & Richard Sustich	*Nanotechnology Applications for Clean Water* (2009)
9780815515876	Rolf Wüthrich	*Micromachining Using Electrochemical Discharge Phenomenon* (2009)
9780815515791	Matthias Worgull	*Hot Embossing* (2009)
9780815515838	Waqar Ahmed & M.J. Jackson	*Emerging Nanotechnologies for Manufacturing* (2009)
9780080964546	Richard Leach	*Fundamental Principles of Engineering Nanometrology* (2009)
9780815520238	Jeremy Ramsden	*Applied Nanotechnology* (2009)
9780815515944	Veikko Lindroos, Markku Tilli, Ari Lehto & Teruaki Motooka	*Handbook of Silicon Based MEMS Materials and Technologies* (2010)
9780815515869	Matthew Hull & Diana Bowman	*Nanotechnology Environmental Health and Safety* (2009)
9781437778236	Yugang Sun & John Rogers	*Semiconductor Nanomaterials for Flexible Technologies* (2010)
9781437778403	Victor Zhirnov & Ralph K. Cavin	*Microsystems for Bioelectronics* (2010)
9781437778489	Zeev Zalevsky & Ibrahim Abdulhalim	*Integrated Nanophotonic Devices* (2010)
9780815515456	Yi Qin	*Micromanufacturing Engineering and Technology* (2010)
9780080964478	Jeremy Ramsden	*Nanotechnology: An Introduction* (2011)
9780815515821	Regina Luttge	*Microfabrication for Industrial Applications* (2011)

Forthcoming Title

9781455778621	Karthikeyan Subramani & Waqar Ahmed	*Emerging Nanotechnologies in Dentistry* (2012)